Electronic Supplementary Information

Small, neutral molecular carriers for selective carboxylate transport

Cally J. E. Haynes, Stuart N. Berry, Joachim Garric, Julie Herniman, Jennifer R. Hiscock, Isabelle L. Kirby, Mark E. Light, Gregory Perkes and Philip A. Gale

Table of Contents

S1. General Remarks

^{1}H NMR (300 MHz) and ^{13}C{^{1}H} NMR (75 MHz) were determined on a Bruker AV300 spectrometer. Chemical shifts for ^{1}H NMR are reported in parts per million (ppm), calibrated to the solvent peak set. The following abbreviations are used for spin multiplicity: s = singlet, d = doublet, t = triplet, m = multiplet. Chemical shifts for ^{13}C{^{1}H} NMR are reported in ppm, relative to the central line of a septet at δ = 39.52 ppm for DMSO-d_6. Infrared (IR) spectra were recorded on a Matterson Satellite (ATR). FTIR are reported in wavenumbers (cm^{-1}). HRMS(ES) spectra were recorded using a Bruker Apex III spectrometer and reported as *m/z* (relative intensity). All solvents and starting materials were purchased from commercial sources and used without further purification unless otherwise stated. Dry DCM was obtained by distillation over CaH_2. Dry pyridine was obtained by distillation over KOH. POPC was supplied by Genzyme. NMR titrations were performed by addition of aliquots of the putative anionic guest as the tetrabutylammonium (TBA) or tetraethylammonium (TEA) salt (0.15 M), in a solution of the receptor (0.01 M) in DMSO-d_6 to 0.01 M solution of the receptor. Tetrabutylammonium carboxylate salts were prepared by reacting the conjugate acid with 1 equivalent of tetrabutylammonium hydroxide (1M in MeOH) in water (1 mL) before removing the solvent.[1] Chloride concentrations during transport experiments were determined using an Accumet chloride selective electrode. HPLC separations were performed on a HP1050 Series system (Agilent Technologies, Palo Alto, CA, USA).

S2. Synthetic procedure

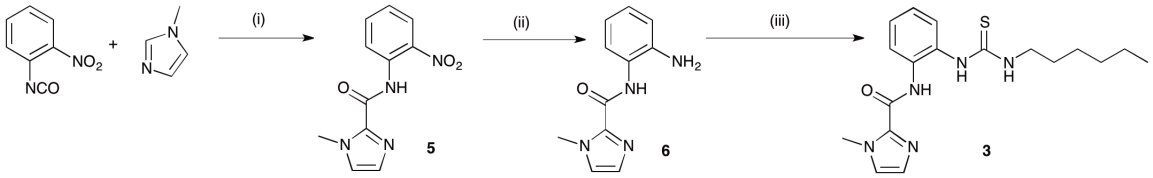

Scheme S1 Reagents and conditions: (i) diphenyl ether, 180 °C, 1 h; (ii) H_2, Pd/C, DMF/AcOH 7.5:1, 12 h; (iii) hexyl isothiocyanate, dry pyridine, 50 °C, 12 h.

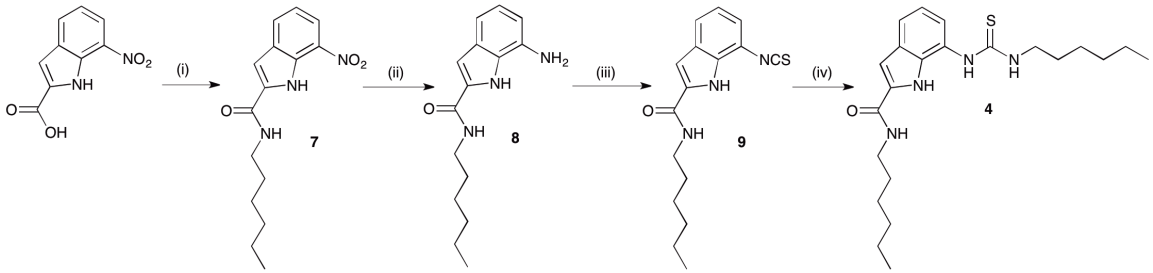

Scheme S2 Reagents and conditions: (i) 1,1'-carbonyldiimidazole, *n*-hexylamine, $CHCl_3$; (ii) H_2. Pd/C, EtOH; (iii) thiophosgene, DCM/ sat. $NaHCO_3$; (iv) *n*-hexylamine, DCM.

1-Methyl-*N*-(2-nitrophenyl)-1*H*-imidazole-2-carboxamide 5

2-Nitrophenyl isocyanate, (2.0g, 12 mmol), was dissolved in 10 mL diphenyl ether and 1-methyl imidazole, (1.1 mL, 13 mmol) was added. The mixture was heated to 180 °C for 1 h and allowed to cool. Subsequent cooling using an ice bath and addition of 250 mL petroleum ether afforded a precipitate, which was filtered and washed with petroleum ether. The yellow- brown solid was purified by flash column chromatography on silica (DCM/ MeOH 1%) to give **5** as a bright yellow solid.

Yield: 1.92 g (65 %); ^{1}H NMR (300 MHz, DMSO-d_6) δ = 11.65, (br s, 1H, NH), 8.52, (m, 1H, aromatic CH), 8.19, (dd, J = 8.42 Hz, 1H, aromatic CH) 7.80, (m, 1H, aromatic CH), 7.53, (br s, 1H, imidazole CH), 7.35, (m, 1H, aromatic CH), 7.16, (br s, 1H, imidazole CH), 4.01, (s, 3H, CH_3); ^{13}C NMR (75 MHz, DMSO-d_6): δ= 157.0 (CO), 138.1 (aromatic CH), 137.8 (aromatic CH), 135.4 (aromatic CH), 133.1 (aromatic CH), 127.9 (aromatic CH), 125.7 (aromatic CH), 124.0 (aromatic CH), 122.4 (aromatic CH), 35.3 (CH_3); Mp: 185 °C; LRMS (ESI+) *m/z*: 247.1 $[M + H]^+$, 269.1 $[M + Na]^+$; HRMS (ES+) *m/z*: $[M + Na]^+$ calculated 269.0651, found 269.0644; IR (film): ν=3280 (amide NH stretching), 1680 (carbonyl C=O stretching).

***N*-(2-Aminophenyl)-1-methyl-1*H*-imidazole-2-carboxamide**, **6**

Compound **5**, (0.3 g, 1.2 mmol), was dissolved in DMF: glacial acetic acid, (15:2, 17 mL). Pd/C, (10 % cat.), was added and the mixture was stirred under atmosphere of H_2 for 5 h, during which time a colour change was observed from yellow to colourless. The Pd/C was removed by filtration through celite and the solvent was removed via reduced pressure distillation. The residue was re-dissolved in DCM and washed with 2 x 100 mL water. The organic phase was dried over $MgSO_4$ and the solvent was removed to give **6** as a white solid.

Assumed 100 % yield; ^{1}H NMR (300 MHz, DMSO-d_6) δ = 9.67, (br s, 1H, NH,), 7.48, (br s, 1H, imidazole CH), 7.41, (m, 1H, aromatic CH), 7.13, (br s, 1H, imidazole CH), 7.00, (m, 1H, aromatic CH), 6.85, (m, 1H, aromatic CH), 6.67, (m, 1H, aromatic CH), 4.92, (br s, NH_2, 2H), 4.04, (s, CH_3, 3H).

***N*-(2-(3-hexylthioureido)phenyl)-1-methyl-1*H*-imidazole-2-carboxamide 3**

Compound **6** (1.2 mmol) was dissolved in dry pyridine and hexyl isothiocyanate (170 mg, 1.2 mmol) was added. The reaction was stirred at 50 °C overnight under N_2. The reaction was cooled and poured over 50 mL water. The resulting precipitate was collected by filtration and re-dissolved in 50 mL DCM. The organic phase was washed with 3 x 50 mL water and 3 x 50 mL sat. $NaHCO_3$. The organic phase was dried over $MgSO_4$ and the solvent was removed to give an orange oil. This was triturated in 20 mL diethyl ether to yield a precipitate, which was collected by filtration and dried under vacuum to give **3** as an off white solid.

Yield: 370 mg (86 %); ^{1}H NMR (300 MHz, DMSO-d_6) δ = 9.85, (s, 1H, thiourea NH), 9.13, (br. s, 1H, amide NH), 8.02, (d, J = 8.3 Hz, 1H, aromatic CH) 7.83, (br. s, 1H, thiourea NH), 7.46, (s, 1H, imidazole CH), 7.22, (m, 3H, aromatic CH), 7.05, (s, 1H, imidazole CH), 4.00, (s, 3H, CH_3), 3.38 (br. m, 2H aliphatic CH_2), 1.49 (br. m, 2H, aliphatic CH_2, 1.23 (br. m, 6H, 3 x aliphatic CH_2), 0.84 (m, 3H, aliphatic CH_3); ^{13}C NMR (75 MHz, DMSO-d_6): δ= 181.7 (CS), 156.8 (CO), 138.1 (aromatic CH), 133.7 (aromatic CH), 130.0 (aromatic CH), 127.4 (aromatic CH), 127.1 (aromatic CH), 126.7 (aromatic CH), 122.4 (aromatic CH), 44.3 (NHCH_2) 35.3 (NCH_3), 31.0 (aliphatic CH_2), 28.4 (aliphatic CH_2), 26.0 (aliphatic CH_2), 22.0 (aliphatic CH_2), 13.9 (aliphatic CH_3); Mp: 120 °C; LRMS (ESI+) *m/z*: 360.2 $[M + H]^+$, 382.1 $[M + Na]^+$, 741.2 $[2M + Na]^+$; HRMS (ES+) *m/z*: $[M + Na]^+$ calculated 382.1678, found 382.1672; IR (film): ν=3320 (thiourea NH stretching), 3300 (amide NH stretching), 3100 (thiourea NH stretching), 1680 (carbonyl C=O stretching).

N-hexyl-7-nitro-1H-indole-2-carboxamide 7

7-nitroindole-2-carboxylic acid (0.5 g, 2.4 mmol) and 1,1'-carbonyldiimidazole (0.389 g, 2.4 mmol) was dissolved in chloroform (50 mL). This was refluxed under nitrogen for 3 hours. *n*-hexylamine (0.31 mL, 2.4 mmol) was added and the reaction mixture was heated at reflux for 24 hours. The cooled reaction mixture was washed with 3 x 50 mL water, 3 x 50 mL 0.1 M HCl and and 3 x 50 mL sat. $NaHCO_3$. The organic phase was dried over magnesium sulfate, and the product was purified by flash column chromatography on silica (DCM/ MeOH 2 %) to give **7** as a yellow solid.

Yield: 180 mg (25 %); ^{1}H NMR (300 MHz, DMSO-d_6) δ = 11.29 (s, 1H, indole NH), 8.95 (t, 1H, J = 5.5 Hz, amide NH), 8.21 (m, 2H, aromatic CH), 7.34 (m, 2H, aromatic CH), 3.30 (m overlapping with water peak, 2H, (NH)CH_2), 1.56 (m, 2H, aliphatic CH_2), 1.32 (m, 6H, 3 x aliphatic CH_2), 0.87 (m, 3H, CH_3); ^{13}C NMR (75 MHz, DMSO-d_6): δ = 159.3 (CO), 134.8 (aromatic CH), 133.0 (aromatic CH), 131.0 (aromatic CH), 130.5 (aromatic CH), 128.6 (aromatic CH), 106.0 (aromatic CH), 31.0 (aliphatic CH_2), 29.0 (aliphatic CH_2), 26.2 (aliphatic CH_2), 22.0 (aliphatic CH_2), 13.0 (aliphatic CH_3); Mp: 68 °C LRMS (ESI+) *m/z*: 290.1 $[M + H]^+$; HRMS (ES+) *m/z*: $[M + H]^+$ calculated 290.1505, found 290.1502; IR (film): ν= 3360 (indole NH stretching), 3310 (amide NH stretching), 1630 (carbonyl C=O stretching).

7-amino-N-hexyl-1H-indole-2-carboxamide 8

Compound **7** (0.180 g, 0.6 mmol) and Pd/C (10 % cat.) were suspended in 25 mL EtOH. The flask was evacuated and the mixture placed under a hydrogen atmosphere and stirred for 3 hours until a colour change from yellow to colourless was observed. The catalyst was removed by filtration through celite and the solvent was removed under reduced pressure.

Assumed 100 % yield, reacted immediately.

N-hexyl-7-isothiocyanato-1 H-indole-2-carboxamide 9

Compound **8** (0.6 mmol) was dissolved in a bi-phasic mixture of DCM (20 mL) and saturated $NaHCO_{3\ (aq)}$ (20 mL). Thiophosgene (1 equiv, 0.6 mmol, 0.046 mL) was dissolved in 5 mL DCM and added dropwise to the solution. The reaction mixture was stirred overnight under N_2. The organic phase was washed with water (2 x 50mL) and dried over $MgSO_4$.

Assumed 100 % yield, reacted immediately.

N-hexyl-7-(3-hexylthiouredio)-1H-indole-2carboxamide 4

Compound **9** (0.6 mmol) was dissolved in dry DCM (30 mL) and *n*-hexylamine (0.6 mmol, 0.08 mL) was added. The reaction was refluxed overnight under N_2. On cooling, the reaction mixture was washed with water (3x50mL) and saturated $NaHCO_3$ (2x50mL) and dried over magnesium sulfate. The crude material was purified by flash column chromatography on silica (DCM/ MeOH 7%).

Yield: 225 mg (23 % overall yield);^{1}H NMR (300 MHz, DMSO-d_6): δ =11.09 (s, 1H, indole NH), 9.31 (br. s, 1H thiourea NH), 8.50 (t, 1H, J = 4.5 Hz, amide NH), 7.72 (br. s, 1H, thiourea NH), 7.44 (d, 1H, J=5.7 Hz, aromatic CH), 7.33 (d, 1H, aromatic CH), 7.13 (d, 1H, aromatic CH), 7.01 (t, 1H, J = 5.7 Hz aromatic CH), 3.47 (d, 2H, J = 4.2 Hz aliphatic CH_2), 1.53 (m, 4H, aliphatic CH_2), 1.29 (m, 12H, aliphatic CH_2), 0.87 (m, 6H, aliphatic CH_3);^{13}C NMR (100 MHz, DMSO-d_6) 180.4 (carbonyl CS), 160.5 (carbonyl CO), 132.1 (aromatic C), 128.8 (aromatic C), 120.0 (aromatic C), 118.2 (aromatic C), 103.4 (aromatic C), 31.0 (aliphatic C), 29.1 (aliphatic C), 28.4 (aliphatic C), 26.1 (aliphatic C), 22.0 (aliphatic C), 13.9 (aliphatic C); Mp: 188.7 ^{o}C; LRMS (ESI+) *m/z*: 402.2 $[M+H]^+$; HRMS (ES+) *m/z*: $[M+Na]^+$ calculated 425.2346 found 425.2364; IR (film): v =3352 (indole NH stretching), 3225 (thiourea NH stretching), 1578 (amide C=O carbonyl stretching).

S3. NMR titrations

In all cases, the change in chemical shift of the aromatic adjascent thiourea NH was monitored. The data was fitted to a 1:1 binding model using WinEQNMR 2 to calculate values for the binding constants K_a.[2] All errors on K_a were < 15 % (individual errors are reported in brackets).

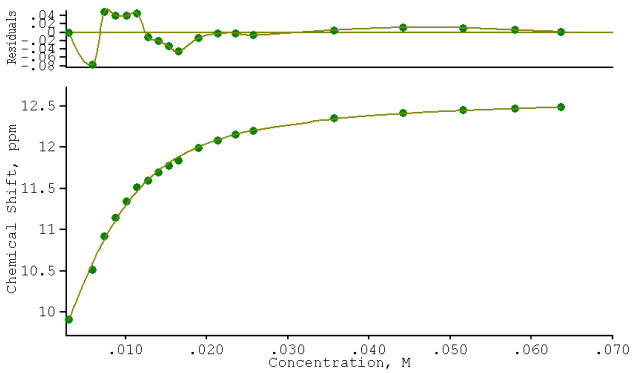

Fig. S1 Binding curve from the ^{1}H NMR titration of receptor **1** with tetrabutylammonium propionate in DMSO-d_6/ H_2O 0.5 % following the thiourea NH resonance at ~9.4 ppm. K_a = 432 M^{-1} (24.20).

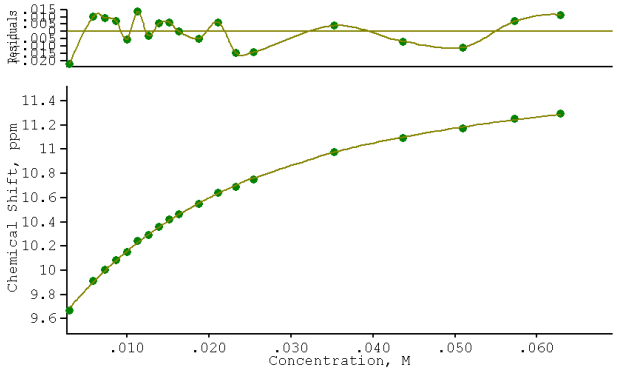

Fig. S2 Binding curve from the ^{1}H NMR titration of receptor **1** with tetrabutylammonium lactate in DMSO-d_6/ H_2O 0.5 % following the thiourea NH resonance at ~9.4 ppm. K_a = 66 M^{-1} (2.284).

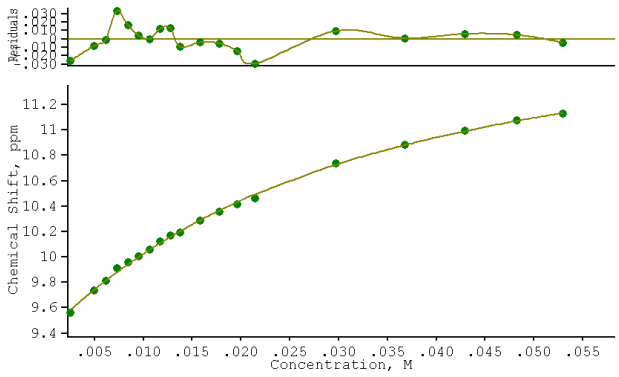

Fig. S3 Binding curve from the ^{1}H NMR titration of receptor **1** with tetrabutylammonium pyruvate in DMSO-d_6/ H_2O 0.5 % following the thiourea NH resonance at ~9.4 ppm. K_a = 42 M^{-1} (2.587).

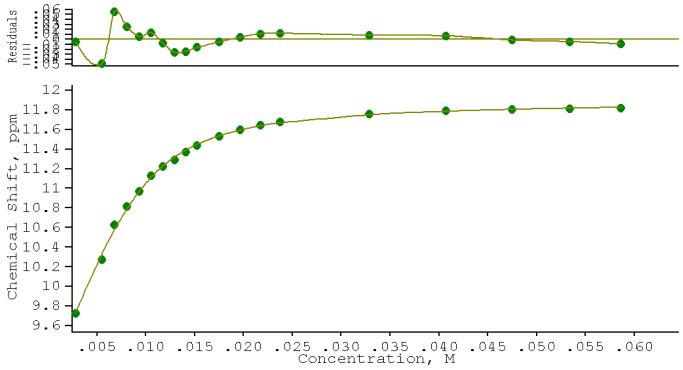

Fig. S4 Binding curve from the ^{1}H NMR titration of receptor **2** with tetrabutylammonium propionate in DMSO-d_6/ H_2O 0.5 % following the thiourea NH resonance at ~9.2 ppm. K_a = 771 M^{-1} (39.50).

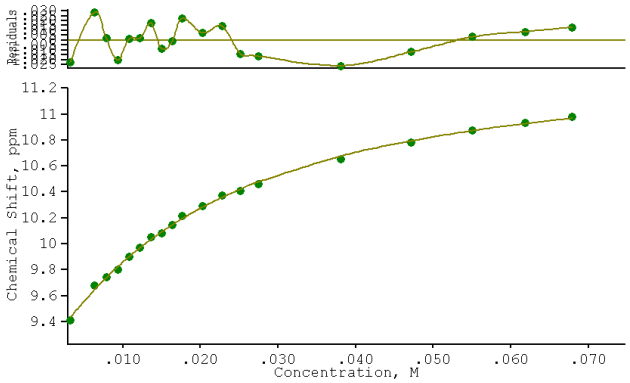

Fig. S5 Binding curve from the ^{1}H NMR titration of receptor **2** with tetrabutylammonium lactate in DMSO-d_6/ H_2O 0.5 % following the thiourea NH resonance at ~9.4 ppm. K_a = 61 M^{-1} (3.344).

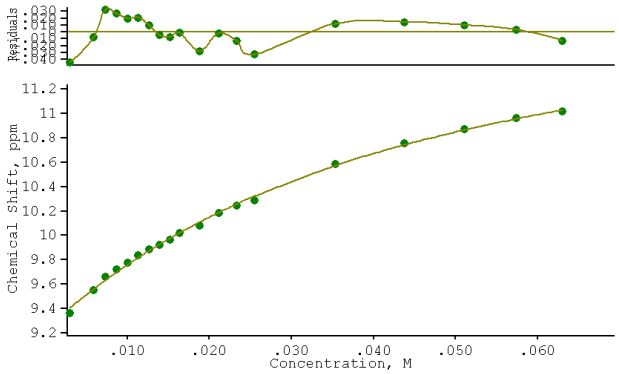

Fig. S6 Binding curve from the ^{1}H NMR titration of receptor **2** with tetrabutylammonium pyruvate in DMSO-d_6/ H_2O 0.5 % following the thiourea NH resonance at ~9.4 ppm. K_a = 28 M^{-1} (2.450).

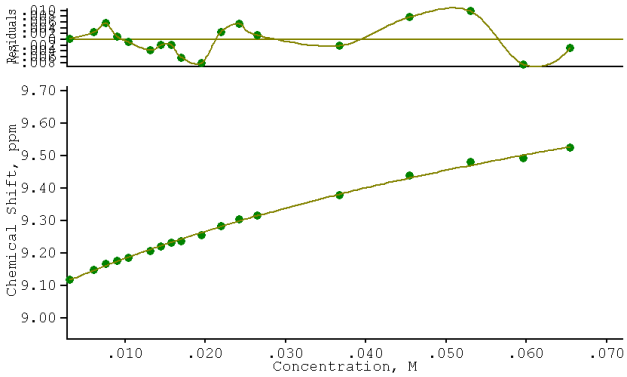

Fig. S7 Binding curve from the ^{1}H NMR titration of receptor **3** with tetrabutylammonium chloride in DMSO-d_6/ H_2O 0.5 % following the thiourea NH resonance at ~9.1 ppm. K_a = 10 M^{-1} (1.282).

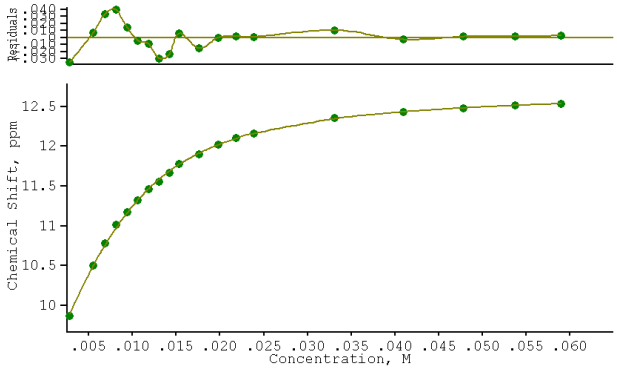

Fig. S8 Binding curve from the ^{1}H NMR titration of receptor **3** with tetrabutylammonium propionate in DMSO-d_6/ H_2O 0.5 % following the thiourea NH resonance at ~9.1 ppm. K_a = 340 M^{-1} (11.00).

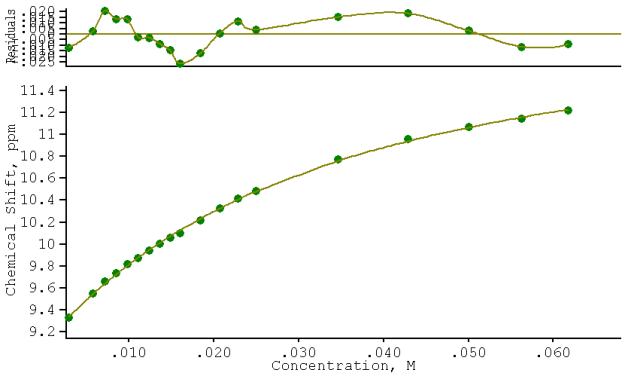

Fig. S9 Binding curve from the ^{1}H NMR titration of receptor **3** with tetrabutylammonium lactate in DMSO-d_6/ H_2O 0.5 % following the thiourea NH resonance at ~9.1 ppm. K_a = 38 M^{-1} (1.615).

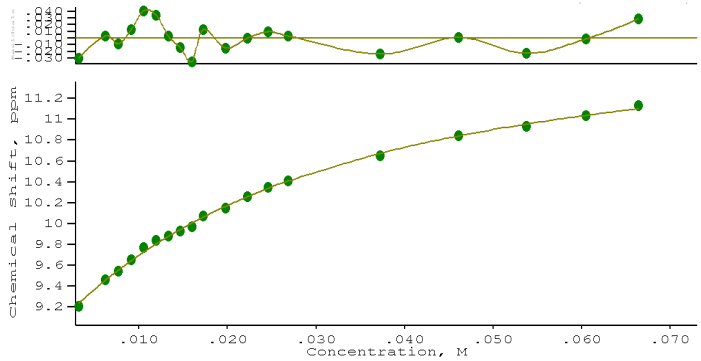

Fig. S10 Binding curve from the ^{1}H NMR titration of receptor **3** with tetrabutylammonium pyruvate in DMSO-d_6/ H_2O 0.5 % following the thiourea NH resonance at ~9.1 ppm. K_a = 42 M^{-1} (2.671).

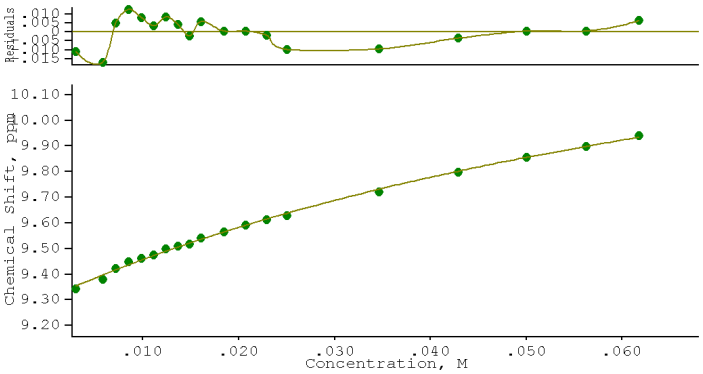

Fig. S11 Binding curve from the ^{1}H NMR titration of receptor **4** with tetrabutylammonium chloride in DMSO-d_6/ H_2O 0.5 % following the thiourea NH resonance at ~9.3 ppm. K_a = 12 M^{-1} (1.470).

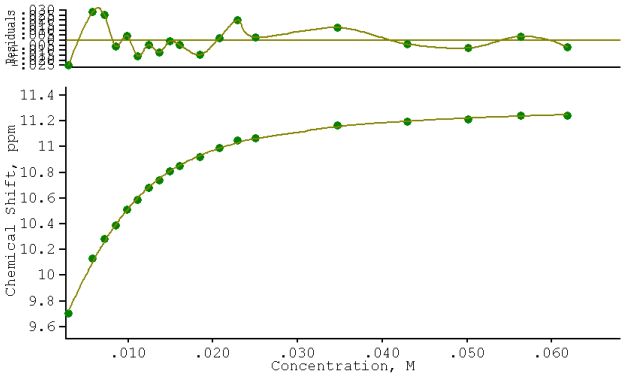

Fig. S12 Binding curve from the ^{1}H NMR titration of receptor **4** with tetraethylammonium bicarbonate in DMSO-d_6/ H_2O 0.5 % following the thiourea NH resonance at ~9.3 ppm. K_a = 389 M^{-1} (16.17).

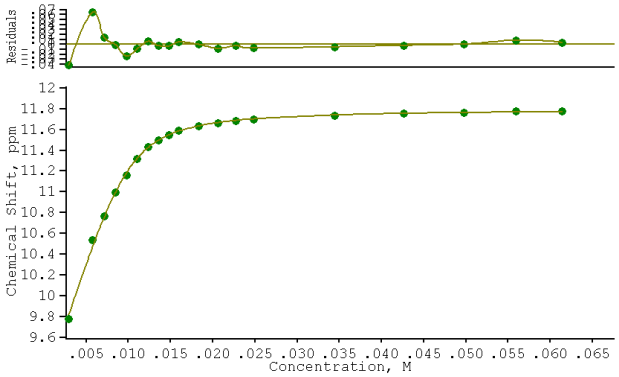

Fig. S13 Binding curve from the ^{1}H NMR titration of receptor **4** with tetrabutylammonium propionate in DMSO-d_6/ H_2O 0.5 % following the thiourea NH resonance at ~9.3 ppm. K_a = 1735 M^{-1} (93.49).

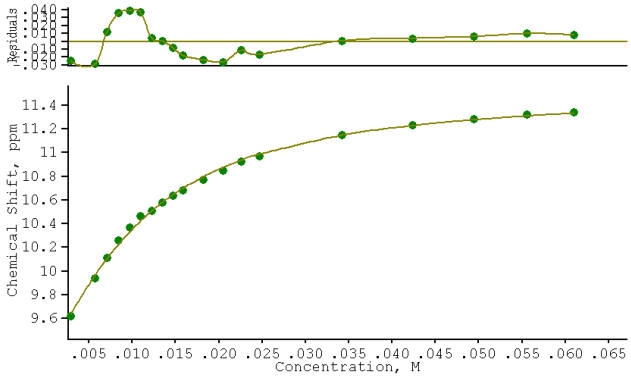

Fig. S14 Binding curve from the ^{1}H NMR titration of receptor **4** with tetrabutylammonium lactate in DMSO-d_6/ H_2O 0.5 % following the thiourea NH resonance at ~9.3 ppm. K_a = 180 M^{-1} (10.34).

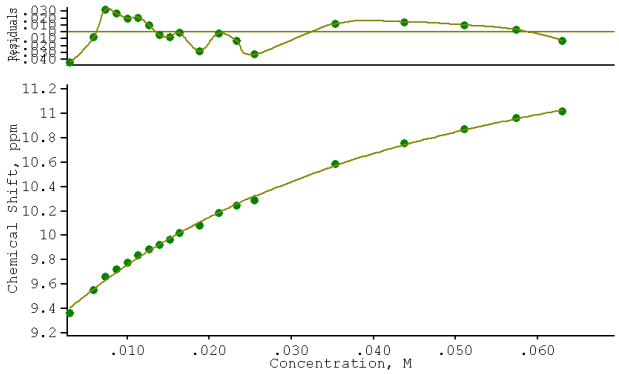

Fig. S15 Binding curve from the ^{1}H NMR titration of receptor **4** with tetrabutylammonium pyruvate in DMSO-d_6/ H_2O 0.5 % following the thiourea NH resonance at ~9.3 ppm. K_a = 90 M^{-1} (5.94).

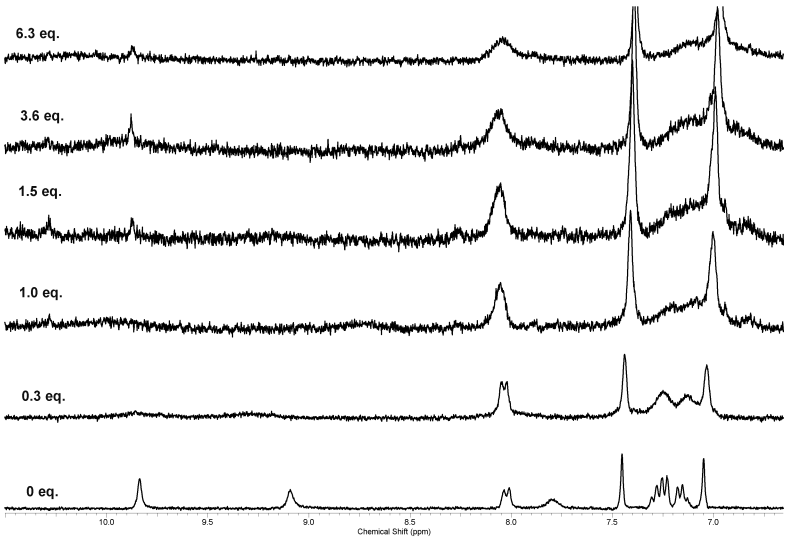

Fig. S16 Stack plot of the aromatic region of the titration of receptor **3** with tetraethylammonium bicarbonate, showing immediate broadening of the NH resonances.

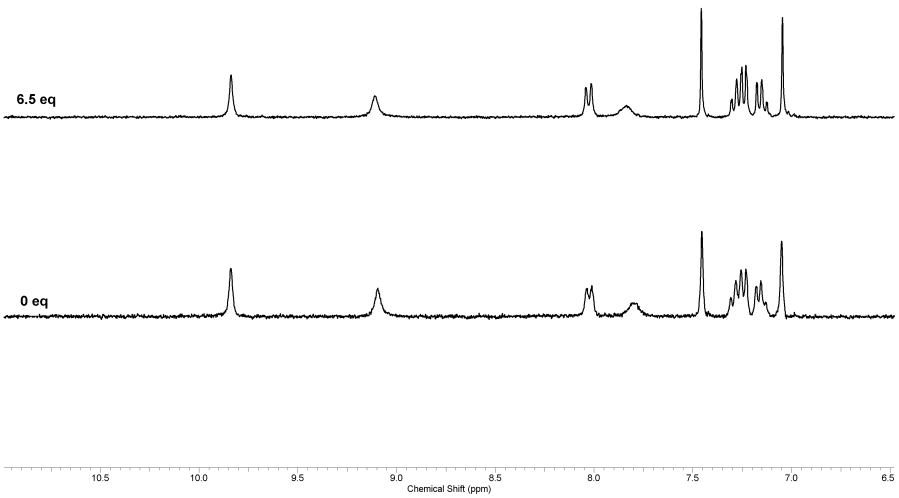

Fig. S17 The aromatic region of the titration of receptor **3** with tetrabutylammonium nitrate, showing no downfield shift of the NH resonances- no interaction detected.

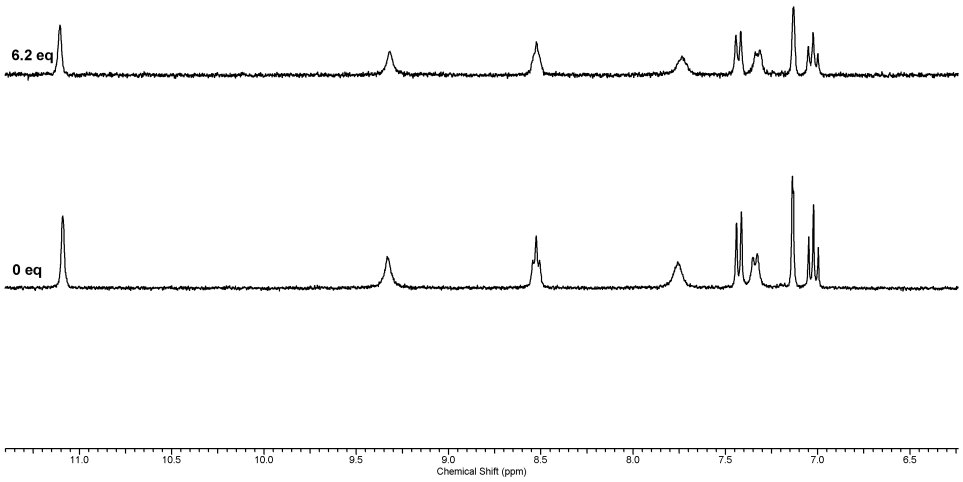

Fig. S18 The aromatic region of the titration of receptor **4** with tetrabutylammonium nitrate, showing no downfield shift of the NH resonances- no interaction detected.

S4. Carboxylate binding profiles

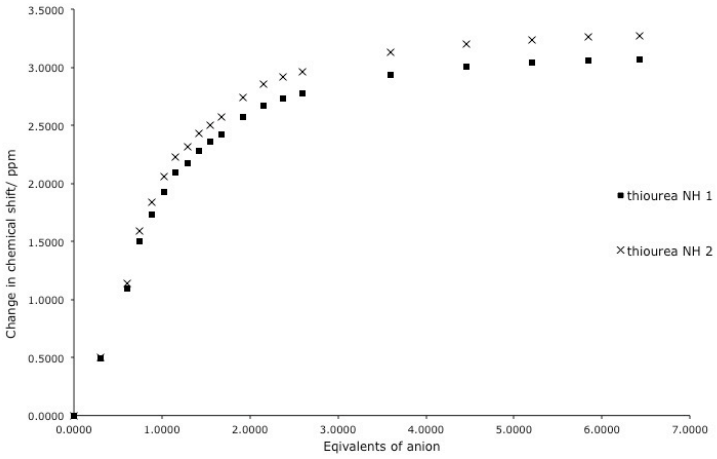

Fig. S19 Change in chemical shift of the NH resonances of receptor **1** on titration with tetrabutylammonium propionate.

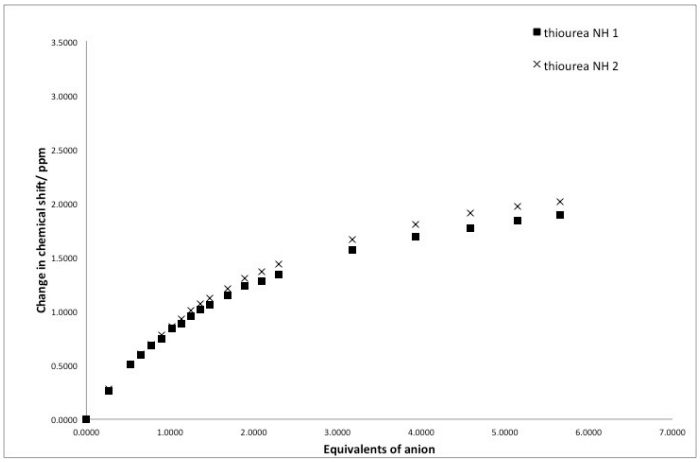

Fig. S20 Change in chemical shift of the NH resonances of receptor **1** on titration with tetrabutylammonium lactate.

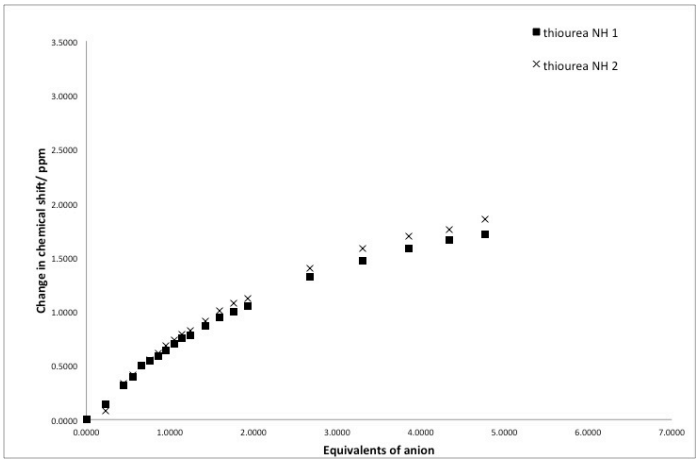

Fig. S21 Change in chemical shift of the NH resonances of receptor **1** on titration with tetrabutylammonium pyruvate.

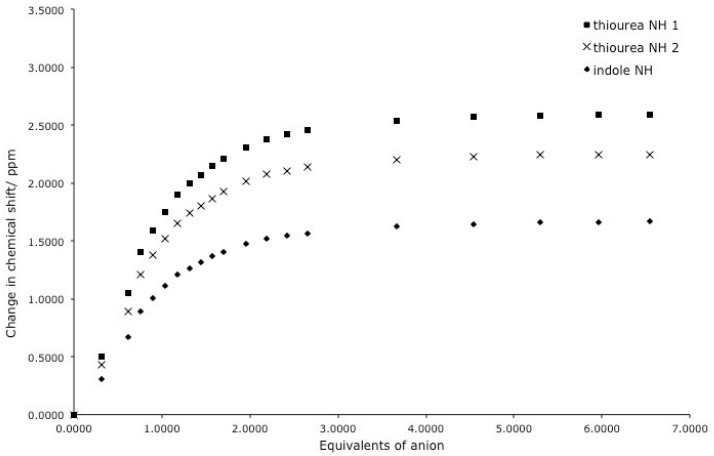

Fig. S22 Change in chemical shift of the NH resonances of receptor **2** on titration with tetrabutylammonium propionate.

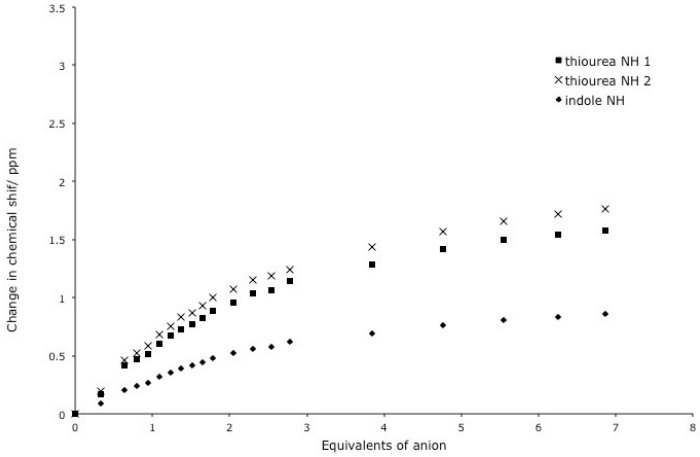

Fig. S23 Change in chemical shift of the NH resonances of receptor **2** on titration with tetrabutylammonium lactate.

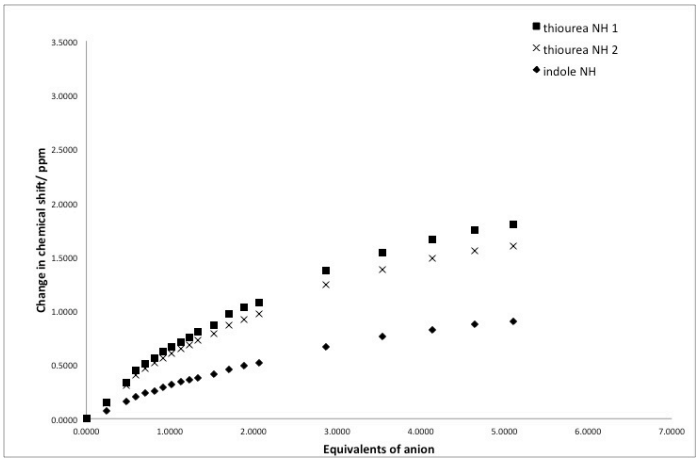

Fig. S24 Change in chemical shift of the NH resonances of receptor **2** on titration with tetrabutylammonium pyruvate.

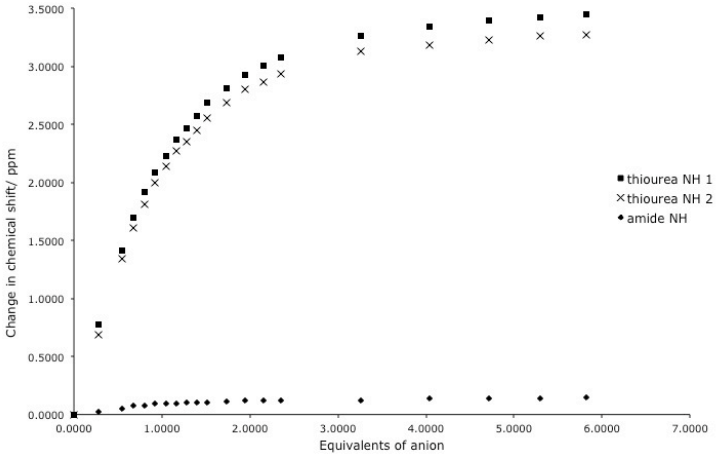

Fig. S25 Change in chemical shift of the NH resonances of receptor **3** on titration with tetrabutylammonium propionate.

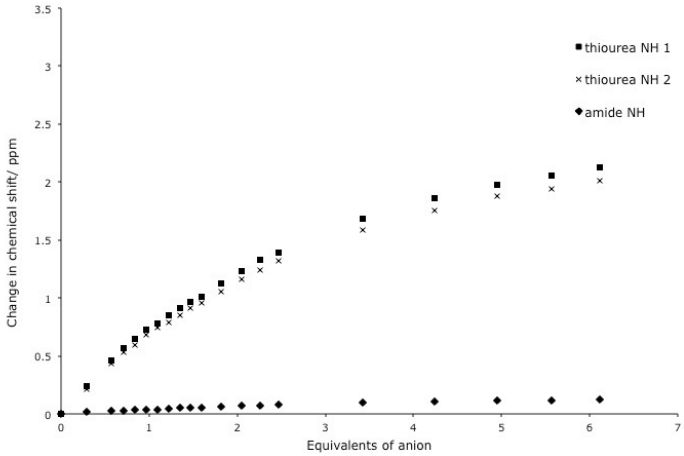

Fig. S26 Change in chemical shift of the NH resonances of receptor **3** on titration with tetrabutylammonium lactate.

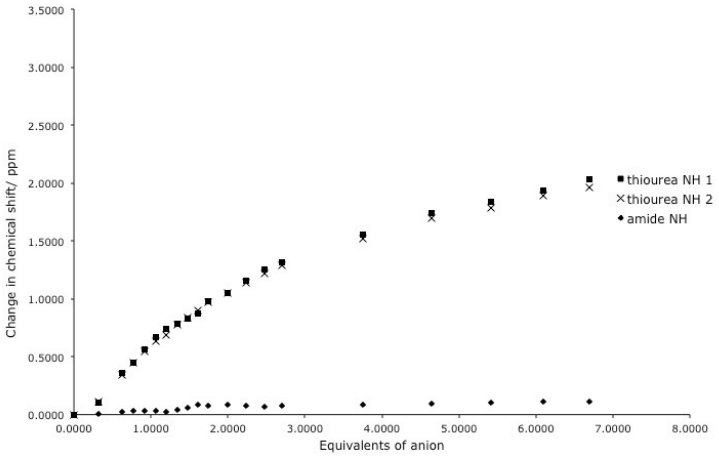

Fig. S27 Change in chemical shift of the NH resonances of receptor **3** on titration with tetrabutylammonium pyruvate.

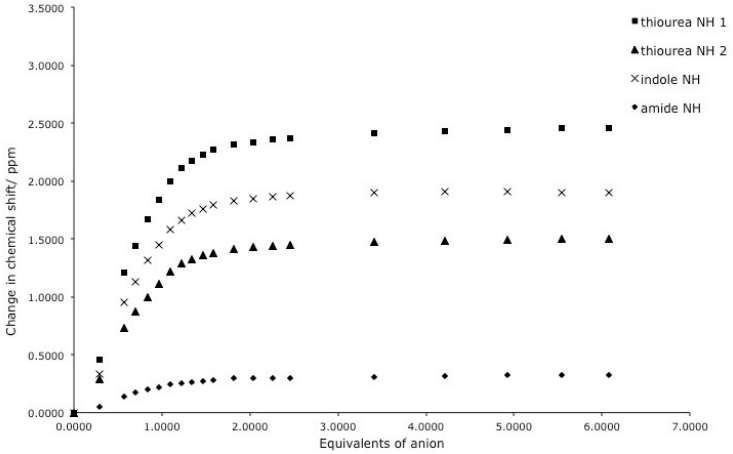

Fig. S28 Change in chemical shift of the NH resonances of receptor **4** on titration with tetrabutylammonium propionate.

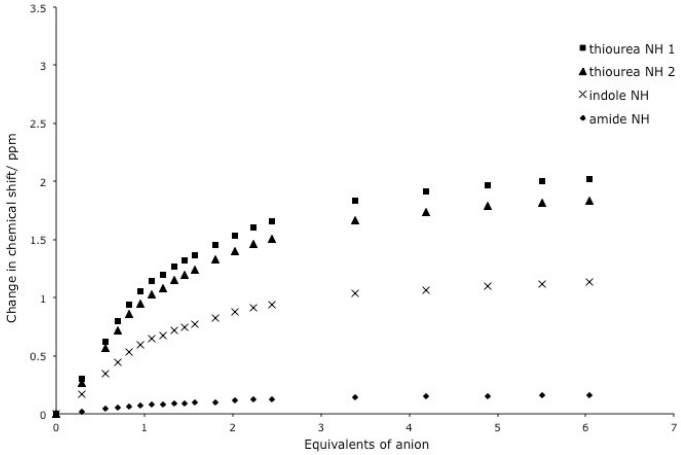

Fig. S29 Change in chemical shift of the NH resonances of receptor **4** on titration with tetrabutylammonium lactate.

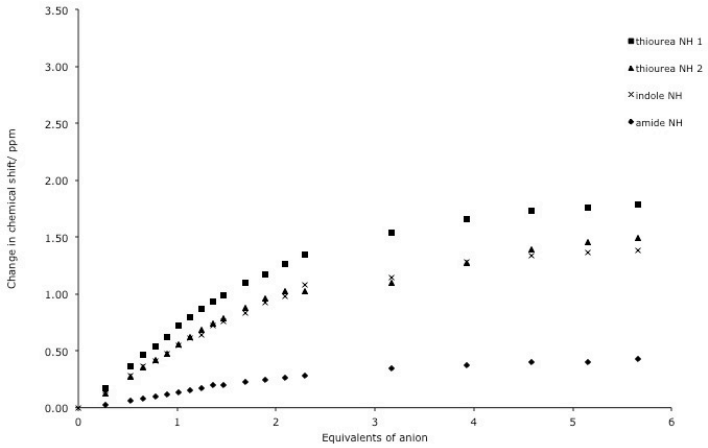

Fig. S30 Change in chemical shift of the NH resonances of receptor **4** on titration with tetrabutylammonium pyruvate.

S5. Anion Transport studies

S5.1 Preparation of Vesicles

A lipid film of 1-palmitoyl-2-oleoyl-*sn*-glycero-3-phosphocholine (POPC) and cholesterol (0% or 30%) was formed from a chloroform solution under reduced pressure and dried under vacuum for at least 6 hours. The lipid film was rehydrated by vortexing with a metal chloride (MCl) salt solution (489 mM MCl, 5 mM phosphate buffer at pH 7.2). The lipid suspension was then subjected to seven freeze-thaw cycles and allowed to age for 30 min at room temperature before extruding 25 times through a 200 nm polycarbonate membrane. The resulting unilamellar vesicles were dialyzed against the external medium to remove unencapsulated MCl salts.

S5.2 Cl^-/NO_3^- antiport experiments

Unilamellar POPC vesicles containing NaCl, prepared as described above, were suspended in 489 mM $NaNO_3$ or 162 mM Na_2SO_4 solution buffered to pH 7.2 with sodium phosphate salts. The lipid concentration per sample was 1 mM. A DMSO solution of the carrier molecule (10 mM) was added to start the experiment and the chloride efflux was monitored using a chloride selective electrode. At 5 min, the vesicles were lysed with 50 μl of octaethyleneglycol monodecylether (0.232 mM in 7:1 water:DMSO v/v) and a total chloride reading was taken at 7 min.

S5.3 Anion pulse experiments

Unilamellar POPC vesicles containing 489 mM NaCl solution buffered to pH 7.2 with 20 mM sodium phosphate salts, prepared as described above, were suspended in 162 mM Na_2SO_4 solution buffered to pH 7.2 with sodium phosphate salts. The lipid concentration per sample was 1 mM. A DMSO solution of the carrier molecule (10 mM) was added to start the experiment and chloride efflux was monitored using a chloride sensitive electrode. At 2 min, a solution of the sodium salt of the anion of interest (1 M in 162 mM Na_2SO_4 buffered to pH 7.2 with 20 mM sodium phosphate salts) was added so that the outer solution contained a 40 mM concentration of that anion. At 7 min, the vesicles were lysed with 50 μl of octaethyleneglycol monodecylether (0.232 mM in 7:1 water:DMSO v/v) and a total chloride reading was taken at 9 min.

S5.4 Cl^-/NO_3^- antiport

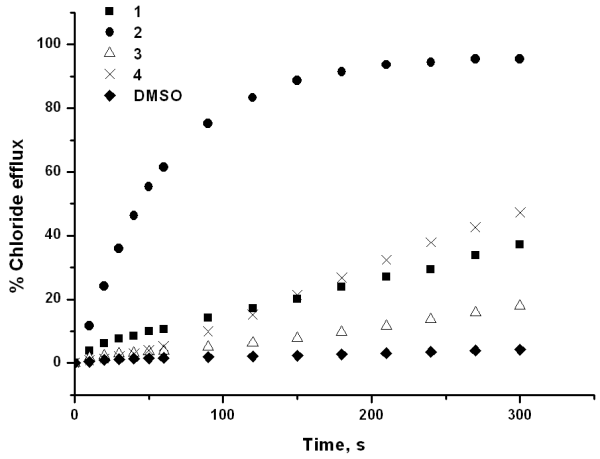

Fig. S31 Chloride efflux promoted by receptors **1**-**4** (2 mol% w.r.t. lipid) from unilamellar POPC vesicles containing 489 mM NaCl buffered to pH 7.2 with 5 mM sodium phosphate salts. The vesicles were suspended in 489 mM $NaNO_3$ buffered to pH 7.2 with 5 mM sodium phosphate salts. At the end of the experiment, the vesicles were lysed in order to calibrate 100 % chloride efflux. Each point represents the average of 3 trials.

S5.5 Anion pulse assay

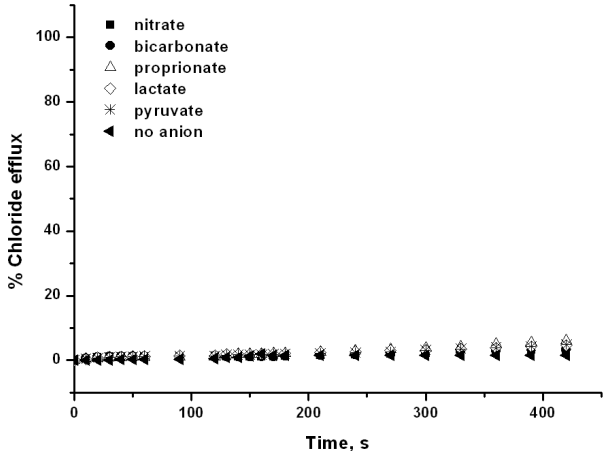

Fig. S32 Chloride efflux on the addition of DMSO (10 μL) from unilamellar POPC vesicles containing 489 mM NaCl buffered to pH 7.2 with 20 mM sodium phosphate salts. The vesicles were suspended in 162 mM Na_2SO_4 buffered to pH 7.2 with 20 mM sodium phosphate salts. At t = 120 s a pulse of sodium anion solution was added such that the final concentration was 40 mM. At the end of the experiment, the vesicles were lysed in order to calibrate 100 % chloride efflux. Each point represents the average of 3 trials.

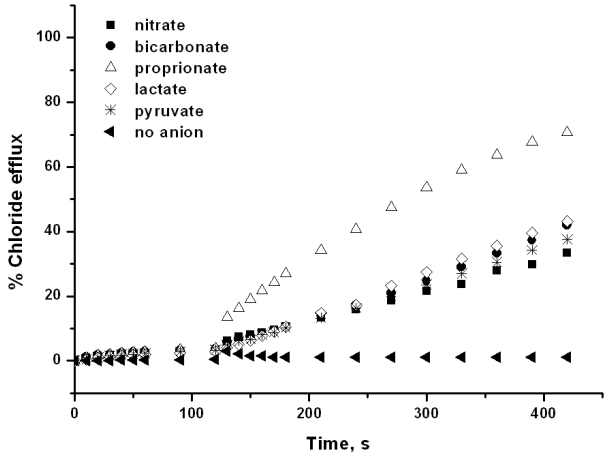

Fig. S33 Chloride efflux promoted by receptor **1** (2 mol% w.r.t. lipid) from unilamellar POPC vesicles containing 489 mM NaCl buffered to pH 7.2 with 20 mM sodium phosphate salts. The vesicles were suspended in 162 mM Na_2SO_4 buffered to pH 7.2 with 20 mM sodium phosphate salts. At t = 120 s a pulse of sodium anion solution was added such that the final concentration was 40 mM. At the end of the experiment, the vesicles were lysed in order to calibrate 100 % chloride efflux. Each point represents the average of 3 trials.

S6. Proof of mobile carrier mechanism

Receptors **1** and **2** have been previously reported as mobile carriers.[3] To ascertain similar proof of mechanism for receptors **3** and **4**, we tested their Cl^-/NO_3^- antiport activity in vesicles composed of POPC/ cholesterol (7:3). It has been suggested that cholesterol reduces the fluidity of the bilayer,[4] thus the rate of transport by mobile carriers may be reduced. The results are shown in Fig. S34 and S35. A reduction in transport rate was observed for receptor **3**, but the activity of receptor **4** was found to *increase*. This is not proof of channel formation and has been observed previously, particularly for receptors with a high *c*logP value.[3a] We therefore investigated the ability of receptor **4** to mediate chloride passage through a U-tube, as it would be impossible for a channel to assemble over such a large distance.[3a, 5] The results, shown in Fig. S36 indicate that receptor **4** was found to mediate chloride transport through an organic nitrobenzene phase, implying that it mobile carrier function.

S6.1 Cholesterol assays

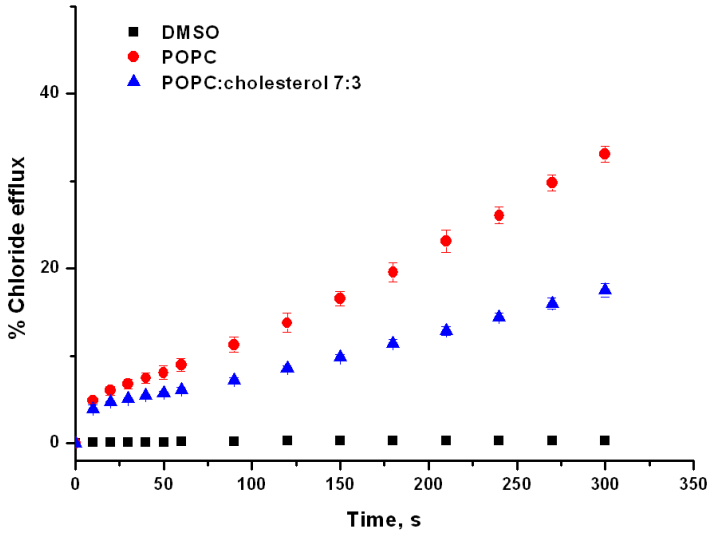

Figure S34 Chloride efflux promoted by receptor **3** (4 mol% w.r.t. lipid) from unilamellar vesicles made from POPC or POPC/ cholesterol (7:3) containing 489 mM NaCl buffered to pH 7.2 with 5 mM sodium phosphate salts. The vesicles were suspended in 489 mM $NaNO_3$ buffered to pH 7.2 with 5 mM sodium phosphate salts. At the end of the experiment, the vesicles were lysed in order to calibrate 100 % chloride efflux. Each point represents the average of 3 trials.

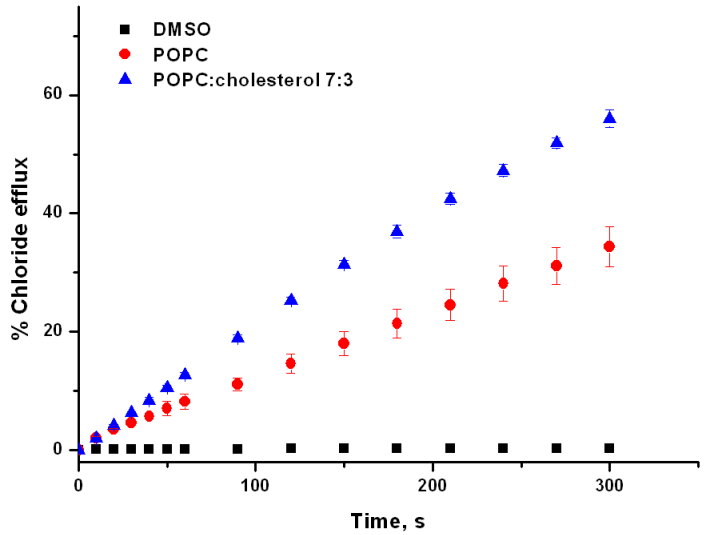

Figure S35 Chloride efflux promoted by receptor **4** (0.5 mol% w.r.t. lipid) from unilamellar vesicles made from POPC or POPC/ cholesterol (7:3) containing 489 mM NaCl buffered to pH 7.2 with 5 mM sodium phosphate salts. The vesicles were suspended in 489 mM $NaNO_3$ buffered to pH 7.2 with 5 mM sodium phosphate salts. At the end of the experiment, the vesicles were lysed in order to calibrate 100 % chloride efflux. Each point represents the average of 3 trials.

S6.2 U-tube protocol

Source phase: 489 mM NaCl buffered to pH 7.2 with 5 mM sodium phosphate salts, 10 mL.
Receiver phase: 489 mM $NaNO_3$ buffered to pH 7.2 with 5 mM sodium phosphate salts, 10 mL.
Organic phase: 1 mM tetrabutylammonium hexafluorophosphate in nitrobenzene with 1 mM receptor **4** (no receptor was added for blank run), 20 mL.

The organic phase was stirred gently at room temperature, and the chloride concentration of the receiver phase was determined using a chloride sensitive electrode (Accumet) after 24 h, 48 h and 120 h.

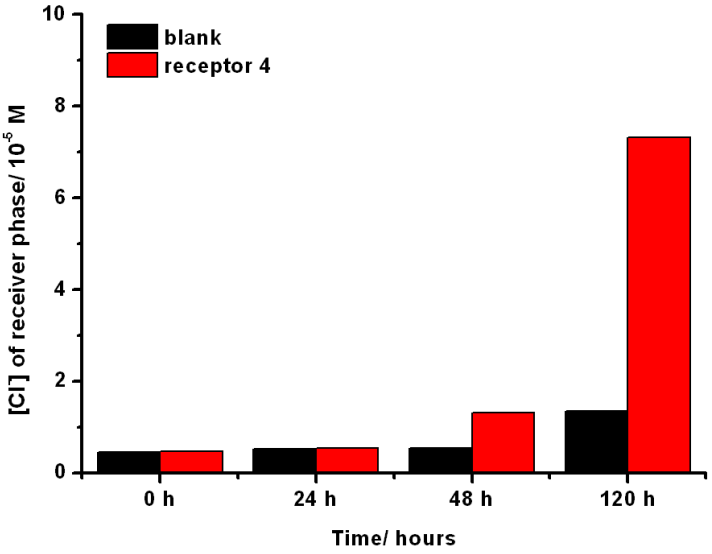

Fig. S36 Chloride concentration of the receiver phase (initial composition 489 mM $NaNO_3$ buffered to pH 7.2 with 5 mM sodium phosphate salts) in a U-tube mobility assay with receptor **4**.

S7. Receptor lipophilicity: HPLC experiments

In order to assess the relative lipophilicity of the receptors studied, we utilised a previously reported HPLC experiment using a reverse phase column, as the retention time on the reverse phase column is related to its lipophilicity.[6]

HPLC separations were performed on a HP1050 Series system (Agilent Technologies, Palo Alto, CA, USA). Samples were injected (10µL) directly onto a Xbridge C18 Column (50mm X 2.1mm 5µm particle size; Waters, Milford, MA, USA) thermostatically controlled at 40°C. The separation was achieved using 20% methanol for 2 minutes followed by a linear gradient to 100% methanol over 10 minutes and held at 100% methanol for 4 minutes at a flow rate of 0.3mL min $^{-1.}$ UV data were recorded at 254nm and mass spectra were recorded using a Platform LC single quadrupole mass spectrometer (Waters, Milford, MA, USA) using positive ion electrospray ionisation (120-1000 *m/z*). The results are shown in table S1.

Table S1 HPLC retention time (min) of receptors **1-4** on a reverse phase column.

Receptor	Retention time (min)
1	11.8
2	12.3
3	11.3
4	13.4

The results were not correlated to calculated values of logP due to the small number of compounds in the series. However, it can be inferred directly from the retention times that receptors **3** and **4** are more lipophilic than parent receptors **1** and **2**. The lipophilicity of the receptors cannot therefore be directly correlated to the anion transport activity; however, given the structural variation across the series this is not unexpected.

S8. Hydrophilicity of carboxylate guests

Literature values for the hydration energy of the carboxylate guests used in this study are not readily available. We hoped to investigate the lipophilicity of the guests as we had done for the receptors in order to investigate which guest presented the biggest energetic barrier to membrane partitioning. However, it has been suggested that this type of HPLC experiments are not reliable for charged species as their behavior on a reverse phase column is more complex,[7] and experimentally we found that the carboxylates exhibited very fast passage through a reverse phase column (performed as reported above and monitored using negative ion electrospray ionisation (120-1000 *m/z*)) with no separation. For these reasons we sought a purely *in silico* measure of the order of hydrophilicity of the carboxylates.

We used Marvin (ChemAxon)[8] and ACD/ I-Lab[9] to calculate a logD (the pH dependent partition coefficient, commonly used for ionizable species) profile and topological polar surface area (TPSA) for each of the carboxylate guests. The results are summarized in table S2.

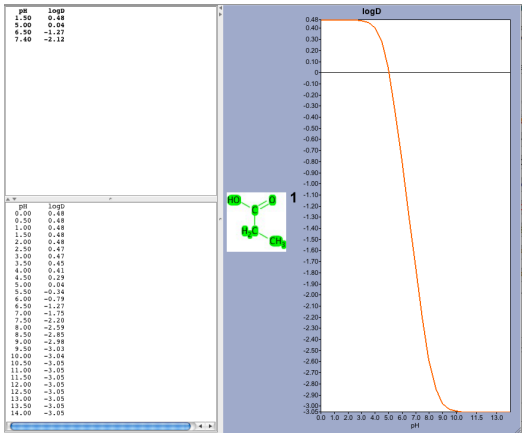

Fig. S37 Propionic acid logD curve calculated using ChemAxon.

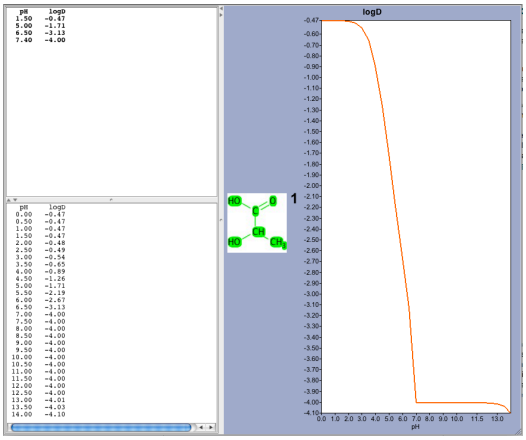

Fig. S38 Lactic acid logD curve calculated using ChemAxon.

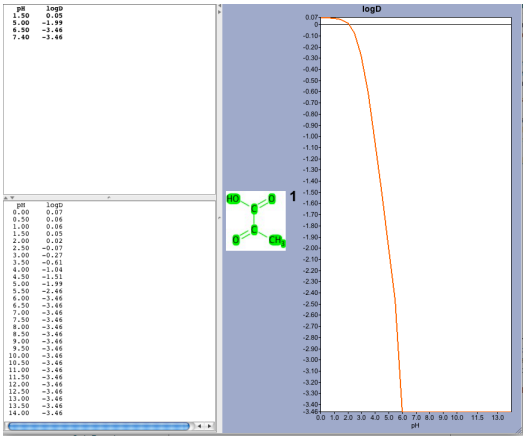

Fig. S39 Pyruvic acid logD curve calculated using ChemAxon.

Table S2 Values of logD and TPSA for the carboxylates used in this study calculated using ChemAxon and ACD/ I-Lab.

Anion	ChemAxon		ACD/ I-Lab	
	logD (pH 7.4)	TPSA / Å^2 (pH 7.4)	logD (pH 7.4)	TPSA / Å^2 (conjugate acid)
Propionate	-2.22	40.13	-2.13	37.30
Lactate	-4.00	60.36	-4.09	57.53
Pyruvate	-3.46	57.20	-4.72	54.37

These values indicate that by both models propionate is found to be the least polar guest species, which is consistent with the transport results which showed that propionate is preferentially transported by all of the receptors studied. However, there is some discrepancy between these models as to whether lactate or pyruvate is the more polar guest species by comparison of the logD (pH 7.4) values. This may be because these two

guests are structurally too similar to distinguish by these methods. Both models agree that the TPSA of lactate is higher than pyruvate.

S9. X-ray crystallography

Crystals of the tetrabutylammonium lactate complex of receptor **2** were grown by slow evaporation of a DMSO solution of the receptor with 6 equivalents of tetrabutylammonium lactate. The structure was elucidated by X-ray crystallography, and is shown in fig. S40. In the solid state, this receptor forms 2:2 complex with lactate. Each lactate anion is coordinated by 3 hydrogen bonds to the thiourea and indole NH groups of one receptor. The lactate anions are coordinated differently by the two inequivalent receptors in this structure. The hydrogen bonding lengths and angles are listed in table S4.

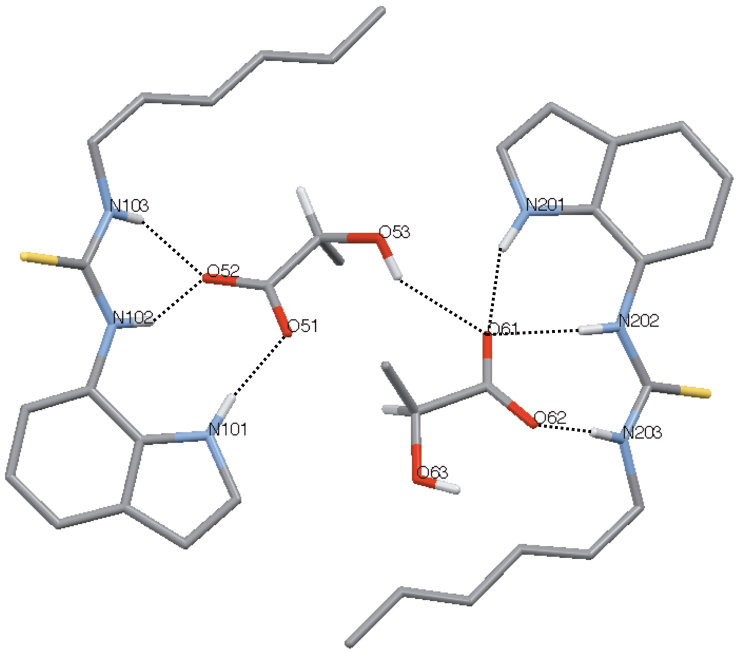

Fig. S40 The X-ray crystal structure of **2**•lactate. Non-acidic hydrogen atoms and tetrabutylammonium counterions have been removed for clarity.

Table S3. Crystal data and structure refinement details.

Identification code	**2012ILK0031**	
Empirical formula	$C_{34}H_{62}N_4O_3S$	
Formula weight	606.94	
Temperature	100(2) K	
Wavelength	0.71075 Å	
Crystal system	Triclinic	
Space group	*P*1	
Unit cell dimensions	a = 8.813(5) Å	α = 105.390(5)°
	b = 13.538(5) Å	β = 100.240(5)°
	c = 17.461(5) Å	γ = 108.830(5)°
Volume	1820.1(13) Å^3	
Z	2	
Density (calculated)	1.107 Mg / m^3	
Absorption coefficient	0.125 mm^{-1}	
F(000)	668	
Crystal	Chip; Colourless	
Crystal size	0.21 × 0.18 × 0.15 mm^3	
θ range for data collection	3.03 – 25.02°	
Index ranges	$-10 \le h \le 8$, $-16 \le k \le 16$, $-20 \le l \le 20$	
Reflections collected	12881	
Independent reflections	9529 [R_{int} = 0.0566]	
Completeness to θ = 25.02°	99.1 %	
Absorption correction	Semi–empirical from equivalents	
Max. and min. transmission	1.000 and 0.777	
Refinement method	Full-matrix least-squares on F^2	
Data / restraints / parameters	9529 / 635 / 490	
Goodness-of-fit on F^2	1.018	
Final R indices [$F^2 > 2\sigma(F^2)$]	$R1$ = 0.0952, $wR2$ = 0.2381	
R indices (all data)	$R1$ = 0.1380, $wR2$ = 0.2861	
Absolute structure parameter	0.13(17)	
Largest diff. peak and hole	1.311 and –0.514 e Å^{-3}	

Diffractometer: *Rigaku AFC12* goniometer equipped with an enhanced sensitivity (HG) *Saturn724+* detector mounted at the window of an *FR-E+ SuperBright* molybdenum rotating anode generator with HF *Varimax* optics (100µm focus). **Cell determination, Data collection, Data reduction and cell refinement & Absorption correction**: CrystalClear-SM Expert 2.0 r7 (Rigaku, 2011) , **Structure solution**: SHELXS97 (G. M. Sheldrick, Acta Cryst. (1990) A**46** 467–473). **Structure refinement**: SHELXL97 (G. M. Sheldrick (1997), University of Göttingen, Germany). **Graphics:** CrystalMaker: a crystal and molecular structures program for Mac and Windows. CrystalMaker Software Ltd, Oxford, England (www.crystalmaker.com)

Special details: All hydrogen atoms were placed in idealised positions and refined using a riding model. The structure is essentially centro-symmetric, and with the exception of the anion (which disorders) will refine well in P-1. However, the anion is enantiomeric L-lactate and therefore the structure as a whole cannot be centro-symmetric. The structure was therefore refined in P1 with non-disordered L-lactate anions, however this resulted in large correlations between pseudo centro-symmetrically related thermal parameters of the receptor and cation molecules. The atomic displacement parameters for chemically identical atom pairs were treated as tied. However, the pseudo symmetry has resulted in a number of Hirshfeld differences. The geometry (1,2 and 1,3 distances) of the L-lactate molecules were restrained.

Table S4 Hydrogen bonding lengths and angles for the crystal structure of **2**•lactate.

D–H···*A*	*d*(*D*–H)	*d*(H···*A*)	*d*(*D*···*A*)	∠(*D*H*A*)
N101–H11···O51^{i}	0.88	1.94	2.7922(14)	162.1
N102–H12···O52^{i}	0.88	2.02	2.8244(11)	151.7
N103–H13···O52^{i}	0.88	2.04	2.8512(12)	153.2
N201–H21···O61	0.88	2.27	3.0396(14)	146.1
N201–H21···O53^{ii}	0.88	2.57	3.1077(13)	120.3
N202–H22···O61	0.88	2.10	2.9797(11)	172.9
N203–H23···O62	0.88	1.92	2.7956(11)	175.0
O53–H53D···O61^{iii}	0.84	2.34	3.0387(13)	140.7
O63–H63D···O62	0.84	2.15	2.6320(13)	116.2

Symmetry transformations used to generate equivalent atoms:
(i) x,y+1,z (ii) x,y,z–1 (iii) x,y,z+1

S10. References

1. J. R. Hiscock, P. A. Gale, N. Lalaoui, M. E. Light and N. J. Wells, *Org. Biomol. Chem.*, 2012, DOI:10.1039/ C2OB26299A.
2. M. J. Hynes, *J. Chem. Soc. Dalton*, 1993, 311-312.
3. a) S. J. Moore, M. Wenzel, M. E. Light, R. Morley, S. J. Bradburry, P. Gomez-Iglesias, V. Soto-Cerrato, R. Perez-Tomas and P. A. Gale, *Chem. Sci.*, 2012, DOI: 10.1039/c1032sc20551c; b) M. Wenzel, M. E. Light, A. P. Davis and P. A. Gale, *Chem. Commun.*, 2011, **47**, 7641-7643.
4. W. F. D. Bennett, J. L. MacCallum and D. P. Tieleman, *J. Am. Chem. Soc.*, 2009, **131**, 1972-1978.
5. N. Busschaert, M. Wenzel, M. E. Light, P. Iglesias-Hernandez, R. Perez-Tomas and P. A. Gale, *J. Am. Chem. Soc.*, 2011, **133**, 14136-14148.
6. a) V. Saggiomo, S. Otto, I. Marques, V. Felix, T. Torroba and R. Quesada, *Chem. Commun.*, 2012, **48**, 5274-5276; b) L.-G. Danielsson and Y.-H. Zhang, *Trends in analytical chemistry*, 1996, **15**, 188-196; c) D. Henry, J. H. Block, J. L. Anderson and G. R. Carlson, *J. Med. Chem.*, 1976, **19**, 619; d) K. Valkó, *J. Chromatogr. A*, 2004, **1037**, 299.
7. R. R. Nadendla, in *Principles Of Organic Medicinal Chemistry*, New Age International Ltd., 2005, pp. 14-31.
8. a) www.chemaxon.com; b) V. N. Vishwanadhan, A. K. Ghose, G. R. Revankar and R. K. Robins, *J. Chem. Inf. Comput. Sci.*, 1989, **29**, 163-172.
9. ACD/ I-Lab, https://ilab.acdlabs.com.